



The Combyn™ ECG: Adding haemodynamic and fluid leads for the ECG. Part II: Prediction of total body water (TBW), extracellular fluid (ECF), ECF overload, fat mass (FM) and “dry” appendicular muscle mass (AppMM)



Falko Skrabal^{a,*}, Georg P. Pichler^a, Mathias Penatzer^a, Johannes Steinbichl^a, Anna-Katharina Hanserl^a, Albrecht Leis^b, Herbert Lobner^c

^a Institute of Cardiovascular and Metabolic Medicine, Mariatrosterstr 67, A 8043 Graz, Austria

^b RESOURCES - Institute of Water, Energy and Sustainability, Department of Isotope Hydrology and Environmental Analytics, Joanneum Research, Elisabethstraße 16/11, A 8010 Graz, Austria

^c Department of Internal Medicine, Krankenhaus Barmherzige Brüder, Marschallgasse 12, A 8020, Graz, Austria

ARTICLE INFO

Article history:

Received 28 June 2016

Revised 27 February 2017

Accepted 4 March 2017

Keywords:

Whole body DXA

Hydration

Dry weight

Sodium bromide

ABSTRACT

Simultaneous with a 12 channel ECG, body composition was analysed by segmental multi-frequency impedance analysis in 101 healthy subjects and in 118 patients with chronic heart failure (CHF, $n=40$), chronic renal failure with haemodialysis (HD, $n=20$), and miscellaneous internal diseases ($n=58$). Whole body DXA and sodium bromide dilution were used as reference methods for total body water (TBW), extracellular fluid (ECF), appendicular muscle mass (AppMM) and fat mass (FM). Empirical prediction equations were developed in a randomized evaluation sample and then evaluated in unknowns. TBW, ECF, AppMM and FM could be predicted with regression coefficients of 0.96, 0.90, 0.95 and 0.93, respectively, all with $p < 0.001$. Only segmental impedances and height, but not age, sex, weight and BMI contributed to the prediction of water compartments. About half the patients with CHF and half of those on HD showed increased ECF/ICF ratio in relation to % FM at the legs but not at the thorax. The predicted AppMM was additionally corrected for increased ECF to determine “dry AppMM”, which is markedly lower than the misleading reference DXA.

This methodology shows promise as a combination of routine ECG with measurement of body composition, assessment of sarcopenia and detection of overhydration.

© 2017 IPEM. Published by Elsevier Ltd. All rights reserved.

1. Introduction

Even today, in the 21st century, traditional clinical signs such as pitting edema, skin fold and ocular bulbar tone, are still used to assess body composition, especially with regard to hydration. Here, the challenge would be to develop physical methods to provide objective, reliable data as a basis for optimal treatment [1,2]. Edema only becomes clinically apparent with an excess of at least 2.5 l

Abbreviations: ACE inhibitors, angiotensin-converting-enzyme inhibitor; AppMM, appendicular muscle mass; AT1 blocker, angiotensin-II-receptor-subtype-1 blocker; BMI, body mass index; BNP, brain natriuretic peptide; CHF, chronic heart failure; CRF, chronic renal failure; DXA, dual energy X-ray absorptiometry; ECF, extracellular fluid; ECG, electrocardiogram; FM, fat mass; HD, haemodialysis; ICF, intracellular fluid; LBM, lean body mass; NYHA, New York Heart Association classification; TBW, total body water.

* Corresponding author. Present address for GPP: Department of Urology, Medical University Graz, Auenbruggerplatz 5/6, A 8036 Graz, Austria

E-mail address: falko.skrabal@medunigraz.at (F. Skrabal).

of extracellular fluid (ECF) [1]. Optimal treatment of chronic heart failure (CHF) or chronic renal failure (CRF) with a haemodialysis [3,4] depends on assessment of dry weight. A means of assessing appendicular muscle mass (AppMM) would be desirable not only in the elderly [5], but in chronic heart and kidney failure as well [6]. When hydration varies, even a gold standard method like whole body DXA can produce misleading results, since it does not differentiate extracellular fluid accumulation from lean mass [7]. So far attempts to detect excess fluid by impedance have only been moderately successful [8,9,10]. In a previous paper [11] we showed that with suitable placement of ECG electrodes, segmental impedance spectroscopy can be used to detect not only over-stretched heart muscle fibres and elevated BNP levels, but also segmental over-hydration in patients with chronic heart failure and effusion in body cavities. In this study, we aimed to predict total body water (TBW), appendicular muscle mass, fat mass (FM), ECF and ECF overload in a mixed sample of 101 healthy subjects and 118 patients with hydration derangement, e.g. in the context

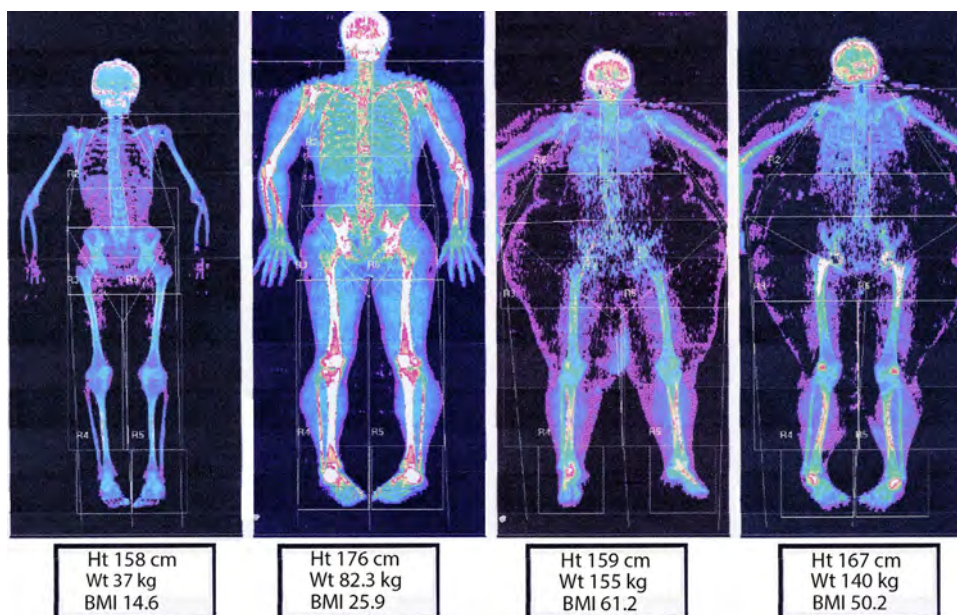


Fig. 1. Extreme examples of pathological body compositions analysed: a male patient with anorexia nervosa (BMI 14.6), an athletic male and two women with morbid obesity and BMIs of 50 and 61 are shown.

of chronic heart failure and long-term haemodialysis for chronic renal failure.

2. Material and methods

2.1. Subjects investigated

Two hundred and nineteen subjects were investigated: the 101 healthy controls were students at our institution or healthy members of a tennis or gymnastic club, or outpatients who were considered healthy after extensive work-up including abdominal and carotid ultrasound, echocardiography and biochemical screening. Consecutive patients referred to the Department of Internal Medicine and to the Institute of Cardiovascular and Metabolic Medicine were asked to volunteer for this study; 118 agreed and were included: 40 patients suffered from CHF due to coronary or hypertensive heart disease, NYHA class II, III, and IV (12, 15 and 13, respectively), and 20 patients from CRF before HD. The remaining patients had more than one diagnosis, so that the total number of diagnoses is greater than the number of patients. The other diagnoses were essential hypertension (13), coronary heart disease without clinical heart failure (12), atherosclerosis (11), chronic kidney disease stage II (24), stage III (22), stage IV (2), cancer (5), celiac disease (4), type II diabetes (3), morbid obesity (6), gastritis (1), chronic pancreatitis (1), type I and II osteoporosis (1), anorexia nervosa (2) and chronic polyarthritis (1). Patients already on treatment continued with their usual medications, including beta-blockers, ACE inhibitors, AT1 blockers, calcium channel blockers, hydrochlorothiazide, loop diuretics and spironolactone. Fig. 1 shows examples of the broad spectrum of subjects and patients included in the present study. The study complies with the Declaration of Helsinki; it was approved by the hospital's ethics committee and all patients gave written informed consent.

2.2. Methods

Patients were instructed to fast for 12 h before their appointments. A blood sample was taken from an antecubital vein to determine background sodium bromide concentrations. One hundred millilitres of tap water containing 676 mg sodium bromide were

administered orally. To avoid additional sources of error, the doses were not normalized to body weight. After 4 h a second blood sample was taken. We measured height (Ht) to the nearest centimetre with a caliper while the subjects were standing and weight (Wt) with an electronic scale (Soehnle No. 7347) to the nearest 100 g.

2.3. Impedance measurements

The subjects rested supine with the upper body elevated at a 30° angle for at least 10 min. This position was chosen for the convenience of patients with dyspnea and/or heart failure. Electrodes were applied and the measurements performed as reported in part I of this publication [11] with some simplifications: the position of the electrodes is shown in Fig. 2. The leg and arm electrodes of the conventional ECG were replaced by double band clamp electrodes for the impedance measurements and the ECG. Leg electrodes were placed above the ankles, the arm electrodes above the wrist. The proximal leg electrodes, used in the first part of the paper, were omitted. Two spot adhesive ECG electrodes were applied on the right side of the neck. Current was passed between the outer neck and the outer left leg electrodes to measure the thoracic and abdominal segments, between the outer distal left and right leg electrodes to analyze the leg segments, and between the outer neck and outer arm electrodes for the arm measurements. The silver chloride double band electrodes and standard ECG spot electrodes were moistened with ECG electrode spray. The edge-to-edge distances between the current application and voltage pick-up electrodes were 3 cm.

Definition of the segments: The left thoracic segment was measured diagonally between the inner neck electrode and V4. The left abdominal segment was measured diagonally between V4 and the right leg electrode. The legs were measured alone between the inner neck and the inner leg electrodes using the contra-lateral leg as ionic current conductor. The arms were measured between the inner neck and the inner arm electrodes.

Segmental multi-frequency impedance measurements were performed at 5, 40 and 400 kHz, at the thorax, abdomen and both legs, respectively. These were chosen because evaluation of the data of our first paper [11] showed that these frequencies gave

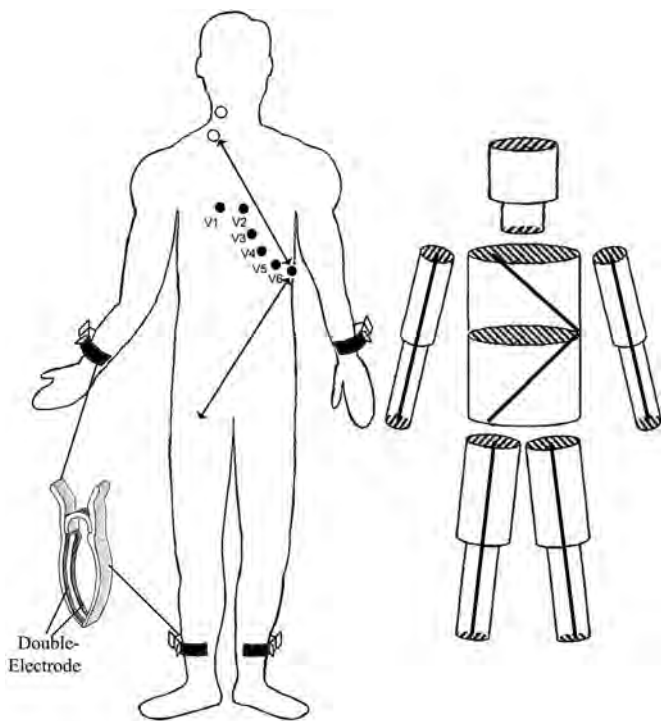


Fig. 2. Placement of the electrodes for the impedance measurements correspond to the placement of the conventional 12-channel ECG with one additional double electrode at the right side of the neck. Thorax and abdomen are measured diagonally between the inner neck electrode and V6, and between V6 and the right groin, respectively. The resulting 6-cylinder-model is shown on the right.

better results than those given by the resistances at Z_{zero} and Z_{∞} calculated from Cole-Cole plots. For the thoracic, abdominal and both leg segments the relations of extracellular to intracellular water (ECF/ICF ratios) were calculated using impedances at 5 kHz (Z_5) and at 400 kHz (Z_{400}) and specific resistances of ECF and ICF as described in the first part of the paper [11]. With this ratio, the variable lengths and the diameters of the respective segments are minimized so that the irregular and unknown cross-sectional areas of the segments are no longer critical. The reproducibility of ECF/ICF ratio measurements was tested in 20 subjects, 1 h apart: Means and coefficients of variations were $99.6 \pm 1.2\%$ and $97 \pm 3.4\%$ for the measurements for the ECF/ICF ratio at the thorax and the legs, respectively.

2.4. Study protocol

2.4.1. Whole body DXA measurements

Whole body DXA (Hologic QDR4500A software version 12.6) was performed in fasting subjects between 8 a.m. and 10 a.m. as recommended by the manufacturer to measure lean body mass (LBM) and fat mass (FM). To calculate TBW from DXA measurements, lean body masses as derived by DXA were multiplied by a factor of 0.73 [12,13]. We have shown previously that there is perfect agreement between TBW_{DXA} and TBW_{Deut} as measured by deuterium dilution [14].

2.4.2. Analytics

The blood samples were centrifuged at 4000 RPM for 12 min; the supernatant serum was then ultra-filtrated (Amicon Ultra-15, PLTK Ultracel-PL Membrane, 30 kDa, Millipore®) at a speed of 4000 RPM for 25 min. Between 4 and 6 ml of ultra-filtrate was recovered. The samples were stored at -28°C for further analysis.

Table 1
Prediction TBW from segmental impedances.

Model		Standardized coefficients Beta	<i>t</i>	Sig.
11	Constant		2,81	,006
	Height2	,54	12,99	,000
	imp_Both_Arms_5 (Ohm)	-2,27	-3,72	,000
	imp_Both_Arms_400 (Ohm)	2,52	3,29	,002
	imp_Both_Legs_5 (Ohm)	,55	2,73	,008
	imp_Both_Legs_40 (Ohm)	-,71	-3,44	,001
	ECF_ICF_Both_Arms	-,81	-3,25	,002
	imp_TH5 (Ohm)	,51	3,94	,000

Dependent variable: total body water, total $r = 0.96$.

2.4.2.1. Sodium bromide measurements. The concentration of bromide in the serum/water obtained by ultrafiltration of human plasma was measured exactly as described in this journal [14].

2.4.3. Statistics

In our laboratory the analytical variability of ECF_{Br} is $\leq 1.3\%$. The coefficient of variation of the Hologic QDR 4500A DXA instrument is $< 1.5\%$, 1 h apart and $< 2.2\%$, one week apart [15].

TBW_{DXA} , LBM_{DXA} , FM_{DXA} , $FM_{Trunk_{DXA}}$, $AppMM_{DXA}$ and ECF_{Br} were predicted by multiple regression analyses using a stepwise backward procedure. Not all measurements were available in all subjects and the number of subjects in different correlations and other analyses can vary. The respective numbers are given in the figures and tables. Because of multiple testing only p values < 0.01 were considered significant.

2.4.4. Evaluation in an independent test set

To assess how the results of the statistical analysis would generalize to an independent data set, the collective was approximately halved randomly by SPSS (SPSS statistic package, version 18.0) into an evaluation set.

The multiple regression equations were calculated using the backward exclusion of non-significant parameters. Only anthropometric measurements, height (Ht), weight (Wt), BMI, sex, age and impedances were included if they were significant at the $p < 0.01$ level in the multiple regression equations. The standardized regression coefficients are given in Tables 1–4. The initial equations were of the general type:

$$\text{Body compartment} = C \pm (f_1)\text{Sex} \pm (f_3)\text{Age} \pm (f_2)\text{Wt} \pm (f_3)\text{Ht}^2 \pm (f_2)\text{Wt} \pm (f_2)\text{BMI} \pm (f_4)z5_{Th} \pm (f_5)z400_{Th} \pm (f_6)z5_{Abd} \pm (f_7)z400_{Abd} \pm (f_8)z5_{Legs} \pm (f_9)z400_{Legs} \pm (f_{10})z5_{Arms} \pm (f_{11})z400_{Arms} \pm (f_{12})\text{ECF/ICF}_{Legs} \pm (f_{12})\text{ECF/ICF}_{Arms}$$

The standardized coefficients or beta coefficients are the estimates resulting from a regression analysis that have been standardized so that the variances of dependent and independent variables are 1 [16]. From these the

Table 2
Prediction ECF from segmental impedances.

Model		Standardized coefficients Beta	<i>t</i>	Sig.
10	Constant		2,78	,007
	imp_TH400 (Ohm)	-,56	-5,03	,000
	Height	1,19	16,02	,000
	imp_ABD5 (Ohm)	-,21	-2,05	,010
	ECF_ICF_Both_Legs	,23	3,05	,004

Dependent variable: ECFNaBr, total $r = 0.90$

Table 3
Prediction appendicular muscle mass from segmental impedances.

Model		Standardized coefficients Beta	t	Sig.
10	Constant		3,01	,004
	imp_ABD5 (Ohm)	−,12	−3,04	,003
	imp_Both_Arms_5 (Ohm)	−2,01	−2,93	,005
	imp_Both_Arms_400 (Ohm)	2,41	2,81	,007
	ECF_ICF_Thorax	−,17	−3,19	,002
	imp_Both_Legs_400 (Ohm)	−,24	−4,75	,000
	ECF_ICF_Both_Arms	−,93	−3,35	,001
	Height	,52	12,00	,000

Dependent variable: appendicular muscle mass, total $r = 0.95$

Table 4
Prediction total body fat from segmental impedances.

Model		Standardized coefficients Beta	t	Sig.
11	Constant		−7,25	,000
	Height	,72	6,38	,000
	imp_TH5 (Ohm)	−,11	−2,23	,029
	imp_Both_Legs_5 (Ohm)	1,47	2,90	,005
	imp_Both_Legs_40 (Ohm)	−2,78	−2,88	,005
	imp_Both_Legs_400 (Ohm)	1,37	2,84	,006
	ECF_ICF_Abdomen	−1,09	−7,49	,000
	BMI	1,10	18,75	,000

Dependent variable: total body fat, total $r = 0.93$

weighting of the different parameters to the estimation can be considered.

Both Ht and Ht² were offered to the stepwise regression analyses. The values for C, f_1 , f_2 and f_3 , etc. varied markedly depending on the exact configuration and location of the electrodes and only apply to the exact configuration of electrodes and measurement sites as used here. The exact values will therefore have to be determined by any user of the method for the selected equipment, selected electrode type and selected location. The equations, however, are included in the commercially available “Combyn ECG”, which simultaneously provides impedance rheographic signals and the 12-channel routine ECG.

These equations were then applied to the unknown test sample. All statistical calculations were performed with the SPSS statistic package, version 18.0.

ECF/ICF ratios of the measured body segments were analyzed for the left thoracic and left leg segments in relation to % FM as predicted by the derived multiple regression equations. Calculating this ratio cancels out the lengths of the investigated segments, which vary between subjects.

3. Results

Anthropometric data and body compartments assessed by gold-standard methods for male and female subjects were as follows: Age ranged from 16 to 97 years and height from 145 to 196 cm. Body size varied enormously, with weight ranging between 37 and 155 kg, and body mass indices between 14.6 and 61.2. Examples of the biological variation are shown in Fig. 1. Impedances for 5 and 400 kHz ranged between 146.4 and 388.5 and 91.0 and 300.1 at the arms, between 17.1 and 42.6 and 12.4 and 34.1 for the thorax, between 12.7 and 41.8 and 9.1 and 32.2 for the abdomen and between 82.7 and 283.3 and 68.1 and 218.7, for the legs, respectively.

Tables 1–4 show the predictions for TBW, ECF, AppMM and body fat using the backward procedure for exclusion of non-significant parameters. The prediction for water compartments rests entirely on segmental impedance parameters and height. Ht²

gave an improvement over Ht, but only for the estimation of TBW and not for the other compartments. Anthropometric parameters such as weight, waist circumference, BMI, age and sex are excluded as non-significant from analysis of water compartments.

Figs. 3–6 show the correlations between the reference methods and the predicted values for the above compartments in the unknown data set. Bland Altman plots are shown as inserts. TBW, ECF, Appendicular Muscle Mass and FM and can be predicted with useful accuracy, both in healthy subjects and in patients with severe fluid balance disturbances.

Fig. 7 (upper) shows the regression between FM predicted from impedance measurements expressed as percent body weight to the ECF/ICF ratio at two different compartments, the thorax and the legs. There is a positive correlation between predicted FM and ECF/ICF ratio at the thorax in healthy subjects, which is also preserved in patients with CHF (upper left) and patients with CRF on HD (upper right). Fig. 7 (bottom) shows the same results using the FM predicted from multiple segmental impedances (FM_{SegImp}) in relation to the ECF/ICF ratio at the legs. In contrast to the thorax, the relation of ECF/ICF of the legs is markedly disturbed in a considerable percentage of patients with CHF (bottom left) and CRF on HD (bottom right).

Fig. 8 shows the index of AppMM (appendicular muscle mass/height²) as determined by segmental impedances in subjects with an ECF/ICF ratio <27% (top left) and in subjects with an ECF/ICF ratio >29% (top right). Fig. 7 (bottom) shows the same results after normalisation of the ECF/ICF ratio to a mean value of 24%, by dividing the mean normal ECF/ICF ratio of 0.24 by each individual ECF/ICF ratio. The results in patients with a normal ECF/ICF ratio remain unchanged whereas the AppMM decreases considerably after correction for an ECF excess.

4. Discussion

To date, segmental single frequency [17] and segmental multi-frequency [18,19] impedance measurements have proven more successful than whole body impedance measurements to predict TBW, FM, ECF and appendicular muscle mass. The latter use a five cylinder model of the four extremities and the trunk as a whole. A narrow limit for the estimation of LBM but wider limits for FM were noted for this method [18], as were a bias of −2.5 kg and a proportional bias with underestimation of FM at low FM and overestimation with high FM [18]. Here, we combined the conventional 12-channel ECG with segmental multi-frequency impedance measurements using a six cylinder model, consisting of the four extremities, and the thorax and the abdomen separately, with conventional placement of the ECG electrodes and one additional double neck electrode. The separation of thorax and abdomen seems justified in the light of the completely different composition of the thoracic and abdominal organs. Our prediction of body compartments is based on a black box approach using empirically derived regression equations in a test sample, which were then evaluated in an unknown evaluation sample. Figs. 3–6 demonstrate the excellent prediction of total body water, appendicular muscle and fat mass and a fair prediction of ECF in an unknown mixed test set of healthy subjects and patients with markedly disturbed body composition. The reference method, TBW_{DXA}, appears to give an excellent estimate of TBW since we achieved a perfect fit between TBW_{DXA} and the deuterium dilution method in our previous study [14]. It is conceivable that the correlation coefficient and the confidence limits for the prediction of fat mass are slightly poorer than those for the water compartments. BMI is also included in the prediction equation since a method based on conductivity measurement should perform better for conducting than for “non-conducting” compartments. The prediction of ECF was the poorest (Fig. 4). This may be at least partly the result of inaccuracies of the

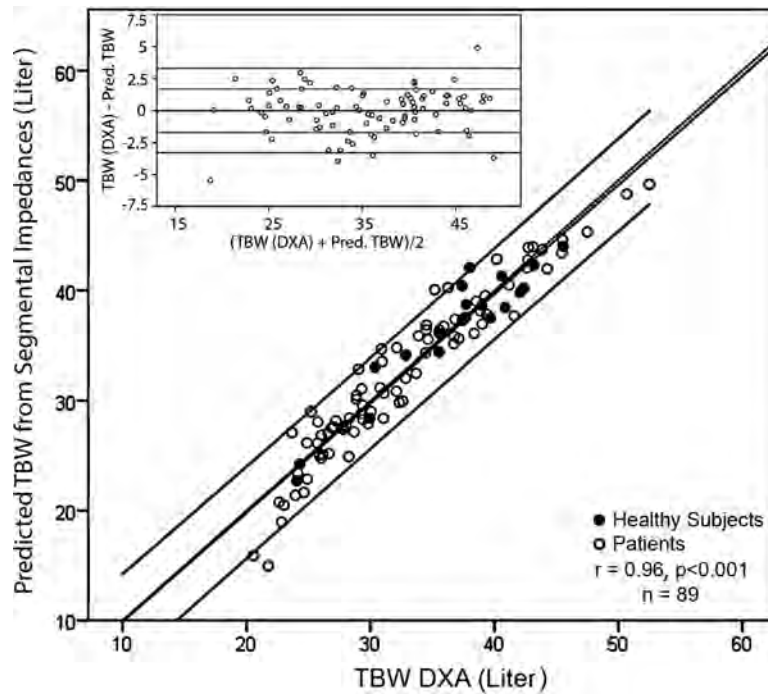


Fig. 3. Prediction of TBW in unknowns: Correlation (Bland-Altman Plot) of TBW as determined from segmental impedances versus DXA analysis. Black dots: healthy subjects, white dots: patients ($n = 89$, $r = 0.96$, $p < 0.001$).

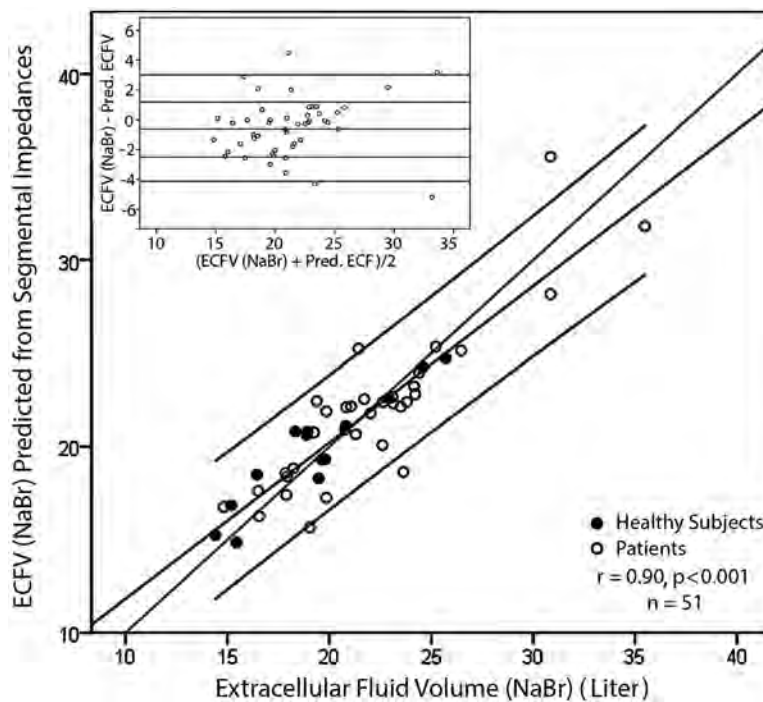


Fig. 4. Prediction of ECF in unknowns: Correlation (Bland-Altman Plot) of ECF as determined from segmental impedances versus NaBr-Dilution analysis. Black dots: healthy subjects, white dots: patients ($n = 51$, $r = 0.90$, $p < 0.001$).

sodium bromide dilution reference method used [20]. Sodium bromide absorption may vary in disease, especially in chronic heart failure, where bowel edema and collagen accumulation in the intestinal wall may delay sodium bromide absorption [21]. Furthermore, ECF may be sequestered away to a third space [22], in the form e.g. of pleural effusions or ascites, where it may not be readily available for rapid exchange with orally administered sodium bromide. This third space of course is accessible to alternating current at all frequencies, and so it may be possible that

the impedance method is even more accurate than the reference method.

It is interesting to note that in the prediction equations, only the segmental impedances at the various frequencies and segments and height² or height contribute to the prediction of water compartments and that the anthropometric parameters such as weight, BMI, waist circumference, age and sex do not. This makes physiological sense since a physically fit elderly woman may have more muscles and body water than a young man who is un-

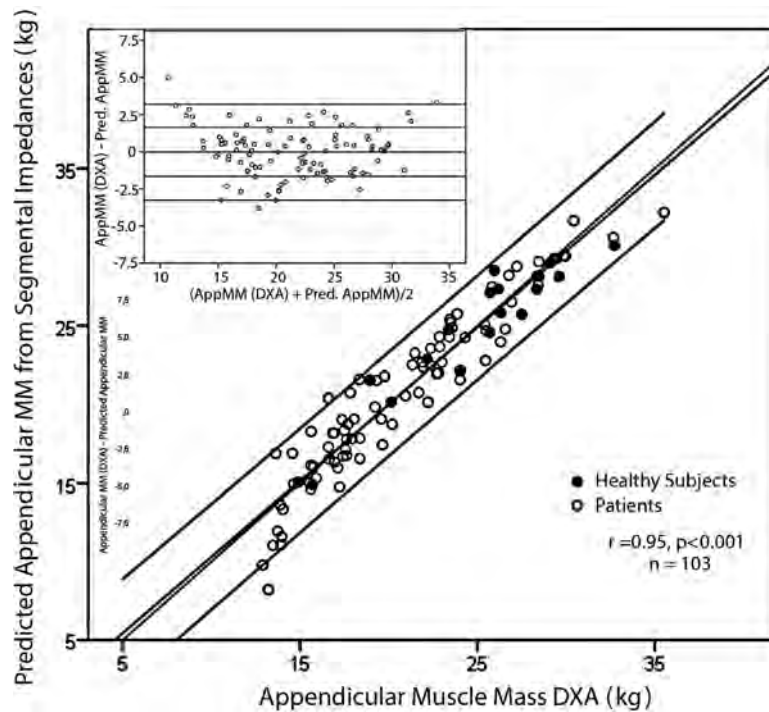


Fig. 5. Prediction of AppMM in unknowns: Correlation (Bland-Altman Plot) of AppMM as determined from segmental impedances versus DXA analysis. Black dots: healthy subjects, white dots: patients ($n = 103$, $r = 0.95$, $p < 0.001$).

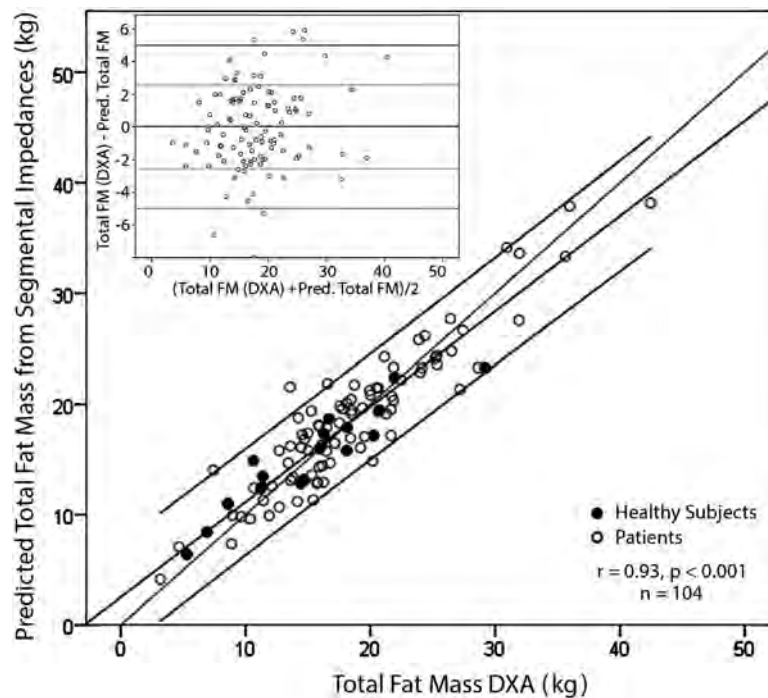


Fig. 6. Prediction of FM in unknowns: Correlation (Bland-Altman Plot) of total FM as determined from segmental impedances versus DXA analysis. Black dots: healthy subjects, white dots: patients ($n = 104$, $r = 0.93$, $p < 0.001$).

fit and seriously ill. We consider this a major step in segmental impedance analysis since these anthropometric parameters are included in previous predictions [18,19], probably only because of the lack of sufficient physiological information provided by measured impedances. We also consider it an important advantage that in our study, the extremity electrodes are applied above the ankles and wrists, where the distribution of fat, water and muscle show representative physiological proportions and that the hands and

feet, consisting mainly of bones, tendons, joint capsules and fibres, are avoided [17,18]. These do not contribute to the compartments of interest and cause major and certainly variable series resistances that cannot fail to falsify the resistances of interest in an unpredictable way.

The prediction of appendicular muscle mass may be especially attractive to tackle the problem of sarcopenia in the elderly and in many chronic diseases. Fig. 5 shows an excellent correlation

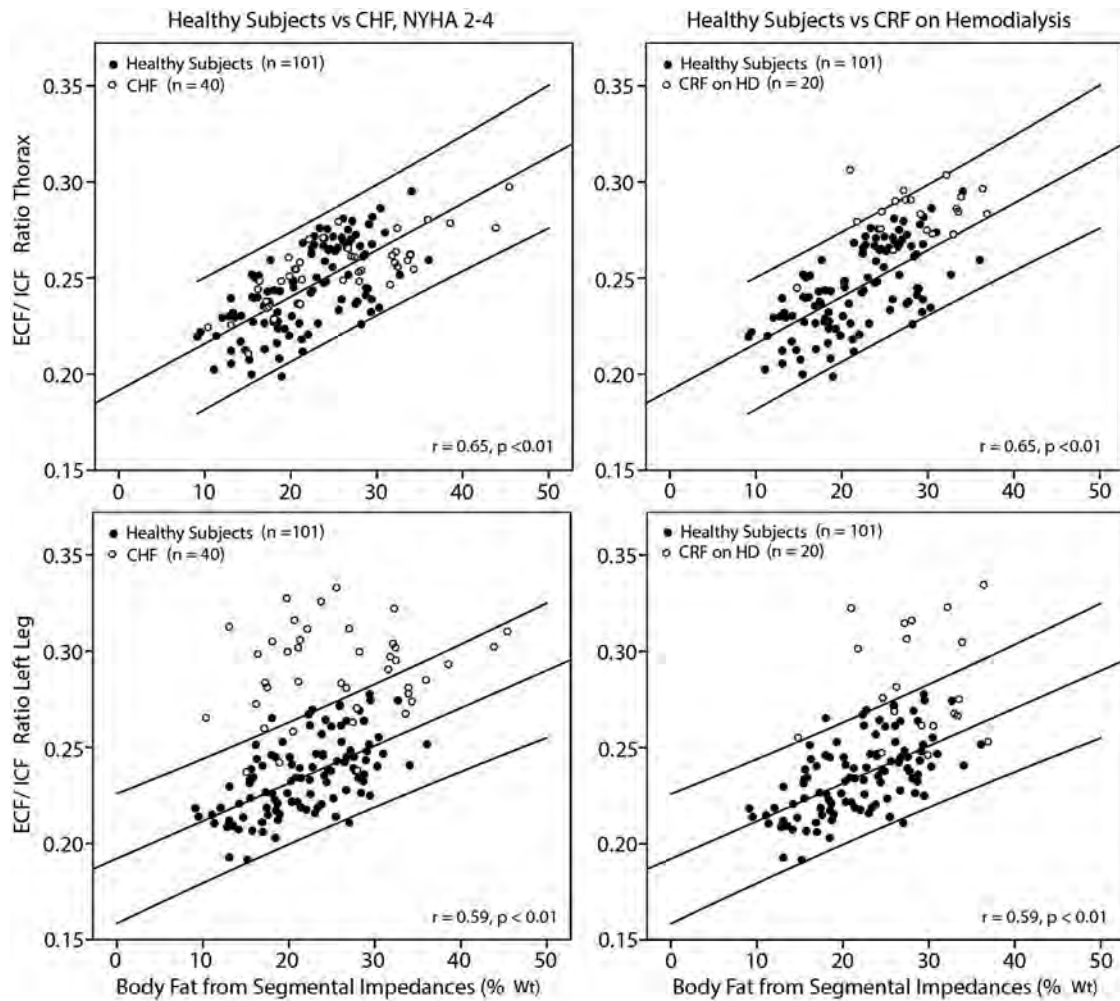


Fig. 7. Relation of impedance predicted FM (wt%) to the ECF/ICF ratios at the thorax (upper) and the left leg (below) in CHF patients (left) and in patients with CRF on hemodialysis (right).

between AppMM as measured by DXA and AppMM predicted by segmental impedance measurements so that segmental multi-frequency impedance measurements can replace whole body DXA in this respect. DXA based results are, however, misleading in edematous states since extracellular water cannot be differentiated from intracellular water in muscle [7]. The impedance based technique shows additional promise for measuring true appendicular muscle mass independent of an excess of extracellular water, since the appendicular muscle mass measured by impedance can be corrected for any hydration changes. The average physiological ECF/ICF ratio of 0.24 (Fig. 8) can be divided by the observed ECF/ICF ratio, and an AppMM adjusted to normal hydration can then be calculated by multiplying the AppMM by the quotient 0.24/actual ECF/ICF. In normally hydrated individuals this quotient is close to one and the results of the AppMM remain the same (see Fig. 8, left). In contrast, in overhydrated subjects, this ratio is markedly lower than one and the AppMM is downsized to the true “dry” AppMM (see right part of Fig. 8).

The clinical use of these methods is still limited by the lack of accurate estimates of the *set point value* for the respective compartments for any individual patient, so it is probable that the results presented in Fig. 7, where we show the regression between FM % weight as calculated from segmental impedances to the ECF/ICF ratios in the different compartments, are more important clinically. This ratio is dimensionless and therefore indepen-

dent of the length and diameter of the investigated segment. The calculations of specific resistivity [9,23,24,25,26,27,28] are controversial and using any one resistivity of them [9] will systematically shift the absolute values but will not affect the biological interpretation since they are applied to all patients uniformly. The impedance values for low and high frequencies are always multiplied by the same factor. Although we found the ECF/ICF ratio to be low, it is interesting to note reports [29] of a similar ratio for extracellular (interstitial) to intracellular water when an isolated organ such as the heart is studied in detail. The higher ECF/ICF ratio in normally hydrated healthy subjects with a higher percentage of body fat (black dots in Fig. 7) can be explained by the fact that intracellular water in fat cells is replaced by fat droplets; this in turn explains the relative increase of ECF in relation to ICF as well as the shift in the relations of ECF to ICF to percent FM [30,31]. Some but not all patients with heart failure or with CRF on chronic intermittent hemodialysis have markedly increased leg ECF/ICF ratios, which could actually indicate higher ECF at this site; however, this relation of % FM to ECF/ICF was undisturbed at the thorax for patients with CHF and CRF (Fig. 7 top), which may indicate that ECF overload is primarily located and detectable at the segments exposed to the highest hydrostatic pressure and not at the thorax. The normal ECF/ICF ratio at the thorax is unsurprising since the use of *intrathoracic* impedance, designed to detect hydration changes in heart failure [32,33], also did not prove to

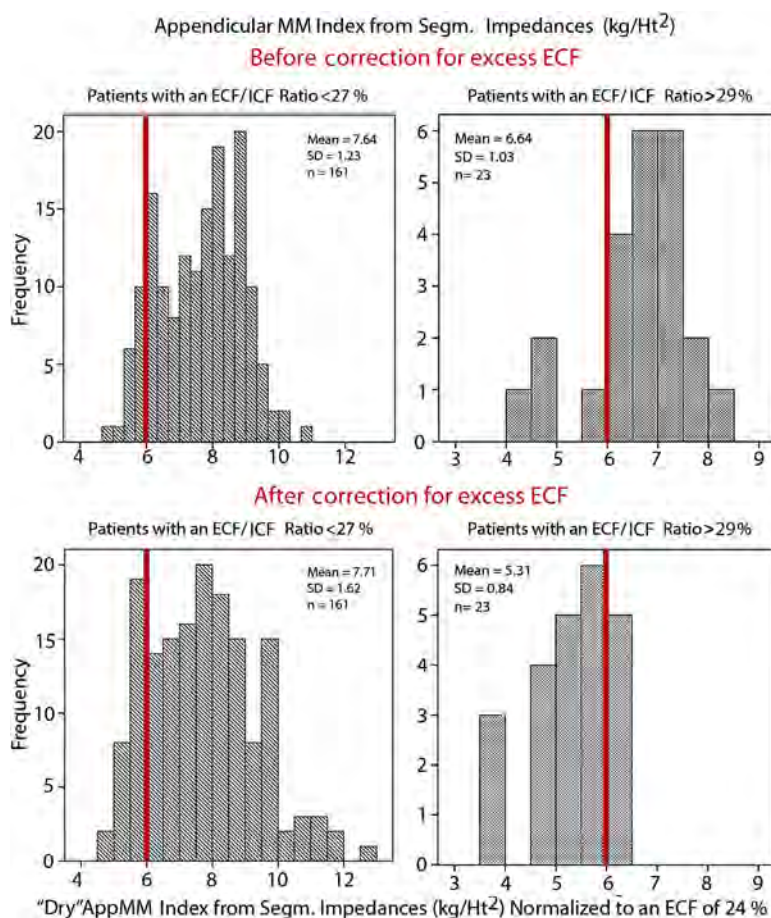


Fig. 8. Impedance predicted AppMM Index uncorrected (upper part of the figure) and impedance predicted AppMM Index corrected for ECF excess (lower part of the figure). The red lines are set at an arbitrary AppMM Index of 6 kg/Ht² to indicate the shift to sarcopenia after correction for excess ECF in over-hydrated patients (compare right upper and lower panel).

be clinically useful, since measuring it did not improve outcome in heart failure patients [34]. These measurements were performed at one frequency at a fixed length between two intrathoracic electrodes. In contrast, in our study the *transthoracic* ECF/ICF ratio was determined at frequencies of 5 and 400 kHz. It can be speculated that the excess of extracellular lung water, which is mainly located within the lung alveoli and not in the vascular bed [35,36,37], may be hidden to low frequency impedance measurements by the lining of the surrounding alveolar cells, which low frequency alternating current may not penetrate. An alternative explanation may be that impedance values of surface applied current at the thorax mainly reflect impedance changes of muscles at the thoracic wall and not that of internal organs like lung and heart [38].

There are also limitations to this work: As we were unable to perform serial measurements after dehydrating patients with fluid overload and after rehydrating patients with dehydration, we do not know how sensitive the methods will be for guiding fluid therapy, which is a logical further goal. We also only used a "black box" model approach to develop multiple regression equations to predict compartments which do not provide substantial new physical data for the interpretation of impedance measurements.

Our study is unique in that it did not focus on predicting body compartments for healthy subjects only, but included patients with drastic differences in body composition associated with diseases such as CHF, and also as shown e.g. in Fig. 1 with a male subject with anorexia nervosa, a healthy athlete and two women with morbid obesity and BMIs over 50. Our aim is to find results that will hold regardless of an individual's health status. To our knowl-

edge this is the first study that measured segmental impedances and not anthropometric parameters to determine the accuracy of the prediction of compartments in disease states. The inclusion of height² or height by the backward regression makes sense since it gives an index of the lengths of the investigated segments, which are a major determinant of the electrical resistances.

Future work will aim to demonstrate that this technology can be used to follow changes of body composition in the individual subject and to determine the "dry weight" of patients with overhydration such as seen in heart failure or in patients on chronic intermittent dialysis. The method will likely be applicable to the assessment of "true" appendicular muscle mass ("dry AppMM"), for which DXA is not appropriate since it cannot differentiate between extracellular and intracellular water. A major advantage is that our method can be performed "piggyback" and simultaneously with a multichannel ECG, since the necessary hardware and software is included in the ECG package of the Combyn™ ECG. There is no need for additional personnel since ECGs are routinely performed with the relevant pathologies. All in all, this will facilitate the transfer of this technology from research into routine clinical use.

Conflicts of interest

F.S. has applied for patents of the methods presented in this paper. The Combyn™ ECG contains all the necessary hardware and software for the 12-channel ECG, segmental multifrequency impedance measurements and finally, also for segmental

impedance rheography. The Combyn™ ECG has received the CE mark in 2016 and will be supplied on request (Institute of Cardiovascular and Metabolic Medicine, Dept. Academic Technologies, A 8043 Graz, Austria, www.ac-tc.at).

Ethical approval

Ethical approval was given by the ethical committee of the Hospital Barmherzige Brüder Graz and by the Medical University Graz No 1254/2015.

Acknowledgements

This work was supported by grant nos. 1.000.034.146 and 1.000.037.669 of the SFG Styria and by grants nos. 849750 and 855562 of the FFG, Austria. We thank Wolfgang Pluhar and Eugenia Lamont for editorial assistance.

References

- Rose BD. Edematous states. Clinical physiology of acid-base and electrolyte disorders. 5th ed. New York: McGraw-Hill; 2001. p. 478–523.
- Alison SB, Lobo DN. Fluid and electrolytes in the elderly. *Curr Opin Clin Nutr Metab Care* 2004;7:27–33.
- Rosner MH, Ronco C. Techniques for the assessment of volume status in patients with end stage renal disease. *Semin Dial Nov-Dec* 2014;27(6):538–41.
- Chazot C, Wabel P, Chamney P, Moissl U, Wieskotten S, Wizemann V. Importance of normohydration for the long-term survival of haemodialysis patients. *Nephrol Dial Transplant Jun* 2012;27(6):2404–10.
- Jansen I, Heymsfield SB, Ross R. Low relative skeletal muscle mass (sarcopenia) in older persons is associated with functional impairment and physical disability. *J Am Geriatr Soc May* 2002;50(5):889–96.
- von Haehling S, Anker SD. Prevalence, incidence and clinical impact of cachexia: facts and numbers-update 2014. *J Cachexia Sarcopenia Muscle Dec* 2014;5(4):261–3.
- Horber FF, Thomi F, Casez JP, Fontelle J, Jaeger P. Impact of hydration status on body composition as measured by dual energy X-ray absorptiometry in normal volunteers and patients on haemodialysis. *Br J Radiol Oct* 1992;65(778):895–900.
- Davies SJ, Davenport A. The role of bioimpedance and biomarkers in helping to aid clinical decision-making of volume assessments in dialysis patients. *Kidney Int Sep* 2014;86(3):489–96.
- Zhu F, Kuhlmann MK, Kaysen GA, Sarkar S, Kaitwatcharachai C, Khilnani R, et al. Segment-specific resistivity improves body fluid volume estimates from bioimpedance spectroscopy in hemodialysis patients. *J Appl Physiol (1985) Feb* 2006;100(2):717–24.
- Raimann JG, Zhu F, Wang J, Thijssen S, Kuhlmann MK, Kotanko P, et al. Comparison of fluid volume estimates in chronic hemodialysis patients by bioimpedance, direct isotopic, and dilution methods. *Kidney Int. Apr* 2014;85(4):898–908.
- Skrabal F, Pichler GP, Gratz G, Holler A. Adding "hemodynamic and fluid leads" to the ECG. Part I: the electrical estimation of BNP, chronic heart failure (CHF) and extracellular fluid (ECF) accumulation. *Med Eng Phys Jul* 2014;36(7):896–904.
- Pace N, Rathbun EN. The body water and chemically combined nitrogen content in relation to fat content. *J Biol Chem* 1945;158:685–91.
- Ritz P. Investigators. Body water spaces and cellular hydration during healthy aging. In: Yasumura S, Wang J, Pierson RN, editors. *In vivo body composition studies*. New York: New York Acad Sciences; 2000. p. 474–83.
- Pichler GP, Amouzadeh-Ghadikolai O, Leis A, Skrabal F. A critical analysis of whole body bioimpedance spectroscopy (BIS) for the estimation of body compartments in health and disease. *Med Eng Phys May* 2013;35(5):616–25.
- Galgani JE, Smith SR, Ravussin E. Assessment of EchoMRI-AH versus dual-energy X-ray absorptiometry to measure human body composition. *Int J Obes* 2011;35:1241–6.
- Schroeder Larry D, Sjoquist David L, Stephan Paula E. Understanding regression analysis. Sage Publications; 1986. ISBN 0-8039-2758-4 p. 31–2.
- Organ LW, Bradham GB, Gore DT, Lozier SL. Segmental bioelectrical impedance analysis: theory and application of a new technique. *J Appl Physiol (1985) Jul* 1994;77(1):98–112.
- Gibson AL, Holmes JC, Desautels RL, Edmonds LB, Nuudi L. Ability of new octapolar bioimpedance spectroscopy analyzers to predict 4-component model percentage body fat in hispanic, black, and white adults. *Am J Clin Nutr* 2008;87:332–8.
- Ling CH, de Craen AJ, Slagboom PE, Gunn DA, Stokkel MP, Westendorp RG. Accuracy of direct segmental multi-frequency bioimpedance analysis in the assessment of total body and segmental body composition in middle-aged adult population. *Clin Nutr Oct* 2011;30(5):610–15.
- Moissl UM, Wabel P, Chamney PW, Bosaeus I, Levin NW, Bosty-Westphal A. Body fluid volume determination via body composition spectroscopy in health and disease. *Physiol Meas* 2006;27:921–33.
- Arutyunov GP, Kostyukevich OI, Serov RA, Rylova NV, Bylova NA. Collagen accumulation and dysfunctional mucosal barrier of the small intestine in patients with chronic heart failure. *Int J Cardiol* 2008;125(2):240–5.
- Ottesen LH, Flyvbjerg A, Jakobsen P, Bendtsen F. The pharmacokinetics of octreotide in cirrhosis and in healthy man. *J Hepatol May* 1997;26(5):1018–25.
- Kay CF, Schwan HP. Specific resistance of body tissues. *Circ Res Nov* 1956;4(6):664–70.
- Burger HC, van Dongen. Specific electric resistance of body tissues. *Phys Med Biol Apr* 1961;5:431–47.
- Rush S, Abildskov JA, McFeer R. Resistivity of body tissues at low frequencies. *Circ Res. Jan* 1963;12:40–50.
- Geddes LA, Baker LE. The specific resistance of biological material—a compendium of data for the biomedical engineer and physiologist. *Med Biol Eng May* 1967;5(3):271–93.
- Cox-Reijnen PL, Soeters PB. Validation of bio-impedance spectroscopy: effects of degree of obesity and ways of calculating volumes from measured resistance values. *Int J Obes Relat Metab Disord Mar* 2000;24(3):271–80.
- Chumlea WC, Baumgartner RN, Roche AF. Specific resistivity used to estimate fat-free mass from segmental body measures of bioelectric impedance. *Am J Clin Nutr Jul* 1988;48(1):7–15.
- Polimeni PI. Extracellular space and ionic distribution in the rat ventricle. *Am J Physiol Sep* 1974;227(3):676–83.
- Martin AD, Daniel MZ, Drinkwater DT, Clarys JP. Adipose tissue density, estimated adipose lipid fraction and whole body adiposity in male cadavers. *Int J Obes Relat Metab Disord Feb* 1994;18(2):79–83.
- Chamney PW, Wabel P, Moissl UM, Müller MJ, Bosty-Westphal A, Korth O. A whole-body model to distinguish excess fluid from the hydration of major body tissues. *Am J Clin Nutr Jan* 2007;85(1):80–9.
- Ganion V, Rhodes M, Stadler RW. Intrathoracic impedance to monitor heart failure status: a comparison of two methods in a chronic heart failure dog model. *Congest Heart Fail Jul-Aug* 2005;11(4):177–81 211.
- Yu CM, Wang L, Chau E, Chan RH, Kong SL, Tang MO, Christensen J, et al. Intrathoracic impedance monitoring in patients with heart failure: correlation with fluid status and feasibility of early warning preceding hospitalization. *Circulation Aug* 2005;112(6):841–8.
- van Veldhuisen DJ, Braunschweig F, Conraads V, Ford I, Cowie MR, Jondeau G. DOT-HF investigators intrathoracic impedance monitoring, audible patient alerts, and outcome in patients with heart failure. *Circulation. Oct* 2011;124(16):1719–26.
- Bossaller C, Schober O, Meyer GJ, Hundeshagen H, Lichtlen PR. Positron emission tomography of regional extravascular lung water and regional pulmonary blood volume in chronic heart failure. *Z Kardiol Jan* 1985;74(1):5–14.
- Grover M, Slutsky RA, Higgins CB, Shabetai R. Extravascular lung water in patients with congestive heart failure. Difference between patients with acute and chronic myocardial disease. *Radiology Jun* 1983;147(3):659–62.
- Kaestle SM, Reich CA, Yin N, Habazettl H, Weimann J, Kuebler WM. Nitric oxide-dependent inhibition of alveolar fluid clearance in hydrostatic lung edema. *Am J Physiol Lung Cell Mol Physiol. Oct* 2007;293(4):L859–69.
- Patterson RP. Can impedance cardiography detect pulmonary edema? In: 16th International Conference on Electrical Bio-Impedance; 17th International Conference on Electrical Impedance Tomography. ICEBI, EIT, June 19–23. Stockholm, Sweden: Book of abstracts; 2016. p. 51.